Modeling of the Stress-Strain Quality of Hydroentangled Nonwoven Fabrics

Sana Ridene
Textile Engineering Laboratory, Monastir University, ISET Ksar Hellal, Tunisia
ridanesana@yahoo.fr

Soumaya Sayeb
Textile Engineering Laboratory, Monastir University, ISET Ksar Hellal, Tunisia
soumaessayeb@yahoo.fr

Houda Helali
Textile Engineering Laboratory, Monastir University, ISET Ksar Hellal, Tunisia
turkihouda@yahoo.fr

Mohamed Ben Hassen
Textile Engineering Laboratory, Monastir University, ISET Ksar Hellal, Tunisia
benrayen@yahoo.fr

Sameer Y. Jaradat
Basic Sciences Department, Imam Abdulrahman Bin Faisal University, Dammam, Saudi Arabia
syjaradat@iau.edu.sa

Ramiz Assaf
Industrial Engineering Department, Faculty of Engineering and Information Technology, An-Najah National University, Palestine
ramizassaf@najah.edu (corresponding author)

Ahmad S. Barham
Department of Chemistry, Faculty of Science, The University of Jordan, Amman, Jordan
ahmad.shawqi@gmail.com

Mohammad Kanan
Jeddah College of Engineering, University of Business and Technology, Jeddah, Saudi Arabia | Mechanical Engineering Department, College of Engineering, Zarqa University, Jordan
m.kanan@ubt.edu.sa (corresponding author)

Received: 11 August 2024 | Revised: 14 September 2024 | Accepted: 19 September 2024

 DOI: https://doi.org/10.48084/etasr.8676

ABSTRACT

Hydroentanglement is a mechanical bonding process designed to produce nonwoven fabrics with appearances and textures that resemble woven and knitted fabrics. Eleven samples of hydroentangled nonwoven fabrics with different compositions and weights were subjected to a series of uniaxial stress-strain tests. Models, ranging from the simple Kelvin to the more complicated Kelvin–Vangheluwe, were fitted to the experimental data to find a generalized and universal model. In this model, a nonwoven fabric was considered a nonlinear viscoelastic material. The combination of Kelvin and Vangheluwe models resulted in an excellent fit to the uniaxial stress-strain curves. The model-predicted results almost overlapped with the experimental data, an indication of its excellent accuracy in predicting the mechanical behavior of nonwoven fabrics.

Keywords-nonwoven; viscoelastic behavior; rheological model; tensile test

I. INTRODUCTION

In recent years, the world has witnessed multiple innovations and developments in textile engineering [1, 2]. Nonwoven fabrics are considered one of the most advanced and innovative textile products [3-5]. The non-woven field is undergoing important growth, representing approximately one-third of the textile market. Nonwoven fabrics can be used for many purposes, from the manufacture of disposable products [6-8] to technical applications [9-11]. During COVID-19, there was an increased demand for personal protective nonwoven products [12].

The hydroentanglement process is the fastest-growing production process of nonwoven fabric, with an annual growth rate of 20% [13-15]. This process achieves excellent fabric performance with aesthetics like woven and knitted fabrics [14, 15]. Softness, drape, conformability, and high strength are the main characteristics that make hydroentanglement-processed fabrics unique among nonwoven products [16]. In hydroentanglement, water jets impact the fiber webs, causing them to entangle and be held together by friction forces. The mechanical properties of hydroentangled nonwoven fabrics are related to the degree of fiber entanglement, which depends on the water jet's settings and speed during manufacturing, the fiber characteristics, and the fiber web forming surface. Most of the research on hydroentanglement has focused on experimental studies [13, 17, 18], and few have examined the simulation of hydroentanglement properties using mechanical models.

In [16], hydroentanglement intensity was defined, showing that it depends on applied energy, fiber dimension and properties, and fiber deformation during the process. Experiments showed that fabric strength is linearly correlated with hydroentanglement intensity. In [19], a computational fluid dynamic model was developed for the hydroentanglement process, which was applied to investigate the effect of fiber web thickness on the degree of fiber entanglement. In [20], a formula was established to calculate the tensile strength of the hydroentanglement nonwoven fabric based on its pull-out behavior. In [21], some stress-strain models developed for nonwoven fabrics were applied to hydroentangled nonwoven fabrics. In addition, experimental stress-strain behaviors in uniaxially loaded hydroentangled nonwoven fabrics were compared and analyzed.

Several viscoelastic models have been developed to characterize the mechanical behavior of textile materials such as fiber, yarn, and fabric [22-28]. In [29], it was concluded that Burger's model is suitable for describing the creep behavior of thermally bonded nonwoven fabrics. The studies in [30, 31] proposed rheological models to describe the compression of both geo-nonwoven fabrics and needle-punched nonwoven fabrics. No rheological model has been proposed to describe the behavior of hydroentangled nonwoven fabrics. The behaviors of hydroentangled fabrics, namely thermal-bonded fabrics and needle-punched nonwoven fabrics, differ under tensile strain. Hydroentangled fabrics rely only on interfiber friction like needle-punched structures, but they are more compact due to the difference between needle and water jet effects. Thermal-bonded nonwoven fabrics have limited movement when strained due to the bonding points fused during the bonding process.

This study establishes four viscoelastic models to study the stress-strain response of hydroentangled nonwoven fabrics. To find the best configuration, several tensile test experiments were performed using 11 different nonwoven fabrics. The Origin software was used to examine the fit of data to the theoretical models. The best model fit was obtained by comparing the experimental stress-strain curves with the fitted ones.

II. MATERIALS AND METHODS

To study the mechanical behavior of hydroentangled nonwoven fabrics, tensile tests were carried out using a Lloyd LR5K dynamometer according to the standard ISO 9073-3:1989, which involved applying tension at a constant speed of 100 mm/min to a rectangular fabric sample (25×5cm²). From the software of the dynamometer, it was possible to extract the force-elongation curves that were compared against several rheological models. Table I shows the characteristics of the nonwoven fabrics tested.

TABLE I. CHARACTERISTICS OF THE TESTED NONWOVEN SAMPLES

Nonwoven composition	Designation	Thickness [mm]	Weight [g/m²]
70%Viscose+30%PES	HN1	0.51	50
70%Viscose+30%PES	HN2	0.5	60
70%Viscose+30%PES	HN3	0.68	77
60%Viscose+40%PES	HN4	0.42	40
60%Viscose+40%PES	HN5	0.55	50
50%Viscose+50%PES	HN6	0.58	45
50%Viscose+50%PES	HN7	0.5	50
50%Viscose+50%PES	HN8	0.76	55
50%Viscose+50%PES	HN9	0.73	65
40%Viscose+60%PES	HN10	0.4	40
40%Viscose+60%PES	HN11	0.5	45

The tested fabrics represent the most used hydroentangled nonwoven fabrics in the textile industry (with different compositions and weights). Stress (σ [Pa]) and strain (ε) were defined as follows [20]:

$$\sigma = Force/(width \times thickness) \quad (1)$$

$$\varepsilon = \Delta L/L = (Extension)/(Initial\ length) \quad (2)$$

Relaxation tests were carried out with deformation values of 5, 10, 20, 30, 40, 50, 60, and 70% of the breaking elongation. The time of the relaxation tests was 300 s. The tests were carried out in a conditioned atmosphere at a temperature of 20 ± 2°C and a relative humidity of 65± 2%.

III. RESULTS AND DISCUSSION

A. Characteristics Tests

When nonwoven fabrics are mechanically deformed, distortions at the macroscopic level produce the destruction of fiber interactions (i.e., the fibers become stressed). In general, linear viscoelastic behavior occurs within small deformations when the microstructure is not modified [22]. At large deformations, the viscous behavior becomes more dominant, and nonlinear viscoelastic models are required for close prediction. The degree of nonlinearity and viscosity/elasticity strongly depends on the material compositions that may largely vary as shown in Table I.

1) Tensile Test

Figure 1 presents the tensile curve of the nonwoven fabric with different square weights. For most of the studied fabrics, the stress-strain curve, shown in Figure 2, consists of three zones:

- The first zone of low strength/weak extension corresponds to the applied pre-tension. In this part, the fiber elements are initially rearranged, straightened, and slipped in response to the increasing load. These events result in reducing the specific stress of the structure achieved experimentally.
- The second linear zone shows a complete recovery.
- The third nonlinear zone has an exponential form that starts with a defined constraint threshold. The final part of this zone has the highest slope, at which point the final breakage takes place.

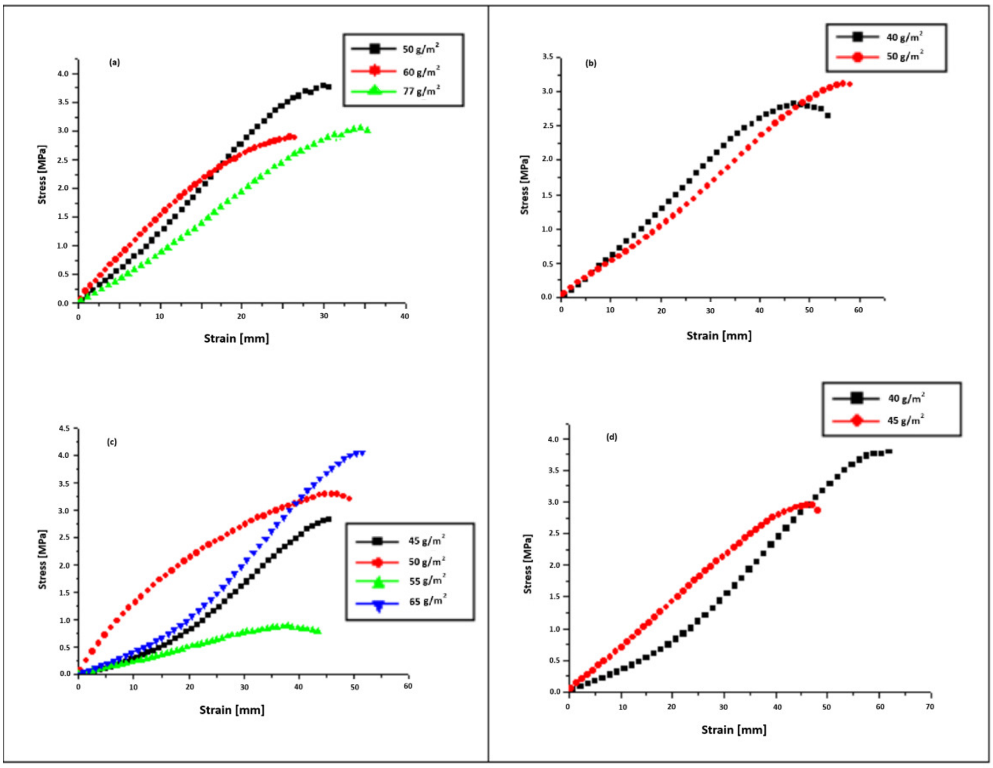

Fig. 1. Hydroentanglement tensile strength for different square weights: (a) 70% Viscose + 30% PES, (b) 60% Viscose + 40% PES, (c) 50% Viscose + 50% PES, and (d) 40% Viscose + 60% PES.

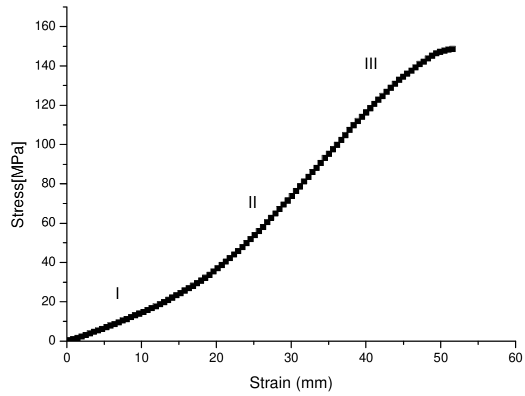

Fig. 2. Tensile curve of hydroentangled nonwoven HN9.

2) Relaxation Test

Figure 3 shows the relaxation test curves standardized by the parameter σ_{max}, which corresponds to the tenacity reached at the end of loading for the different nonwoven fabrics tested. Figure 4 also shows that the relaxation curves of the standardized tenacities are presented in the form of a curved beam. Thus, it can be stipulated that the relaxation of the tenacities depends on the imposed deformation level. Thus, it is confirmed that the nonwoven fabric exhibits viscoelastic behavior. However, according to Figure 4, the tenacity standardized at the relaxation time (t = 300 s) also depends on the imposed deformation level. It is weak-willed during the deformation level (in the first zone of the tensile curve). This parameter becomes more significant in the second zone. Then, it decreases to a minimum (starting from the beginning of the third zone of deformation level during the tensile test). In addition, with regard to the tangent modulus, this parameter follows the same trend as the normalized stress curve. As a result, it can be concluded that nonwoven fabrics present nonlinear viscoelastic behavior [24]. The model describing the mechanical behavior of hydroentangled nonwoven fabric must include a nonlinear component.

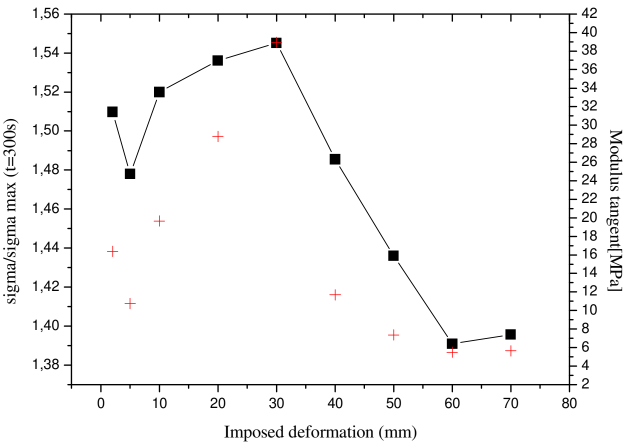

Fig. 3. Relaxation curve of hydro-entanglement nonwoven HN7.

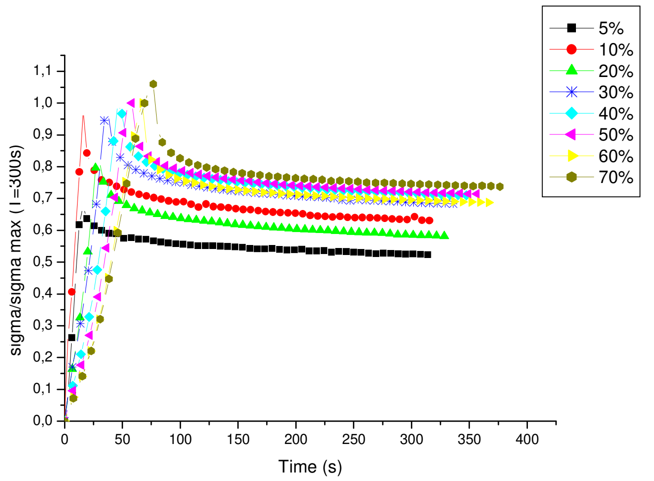

Fig. 4. Evolution of the tenacity standardized at time t =300 s according to the imposed deformation of the hydroentanglement nonwoven HN7

B. Rheological Model

With different combinations of Kelvin, Maxwell, and Vangheluwe elements, several viscoelastic mechanical models were obtained to describe the tensile behavior of nonwoven fabrics [26]. Several viscoelastic properties of nonwoven fabrics during uniaxial loading are presented through the Kelvin model with nonlinear spring, the one-term generalized Vangheluwe model, the two-term generalized Vangheluwe model, and a combination of Vangheluwe and Kelvin elements. The nonlinear spring is assumed to follow the power rule throughout. To investigate the performance of each model, the experimental data were fitted with the derived equations mentioned in Figure 6. The Origin software was used to determine the rheological parameters. The main purpose is to acquire a suitable model for describing the uniaxial behavior of nonwoven fabric. Equations (3) and (4) describe the strain (σ_1 and σ_2) of the Kelvin and the Vangheluwe model [Figure 5 (a, b)] during uniaxial tests, respectively.

$$\sigma_1 = C_k * \varepsilon^2 + \mu_k * \acute{\varepsilon} \quad (3)$$

$$\sigma_2 = \mu_V * \acute{\varepsilon}\,(1 - exp\,((\frac{-E_v}{\mu_v}) * (\frac{\varepsilon}{\acute{\varepsilon}}))) + C_V * \varepsilon^2 \quad (4)$$

To obtain a new model that better fits the experimental data, a combination of the Vangheluwe and Kelvin models was used, as shown in Figure 5 (d). Thus, these equations were expressed as follows:

$$\sigma_3 = \mu_{V1} * \acute{\varepsilon}\left(1 - exp\left(\left(\frac{-E_{v1}}{\mu_{v1}}\right) * \left(\frac{\varepsilon}{\acute{\varepsilon}}\right)\right)\right) + C_{V1} * \varepsilon^2 + \mu_{V2} * \acute{\varepsilon}\,(1 - exp\,((\frac{-E_{v2}}{\mu_{v2}}) * (\frac{\varepsilon}{\acute{\varepsilon}}))) + C_{V2} * \varepsilon^2 \quad (5)$$

$$\sigma_4 = C_k * \varepsilon^2 + \mu_{V1} * \acute{\varepsilon}\left(1 - exp\left(\left(\frac{-E_{v1}}{\mu_{v1}}\right) * \left(\frac{\varepsilon}{\acute{\varepsilon}}\right)\right)\right) + C_{V1} * \varepsilon^2 + \mu_{V2} * \acute{\varepsilon}\left(1 - exp\left(\left(\frac{-Ev2}{\mu v2}\right) * \left(\frac{\varepsilon}{\acute{\varepsilon}}\right)\right)\right) + C_{V2} * \varepsilon^2 + \mu_k * \acute{\varepsilon} \quad (6)$$

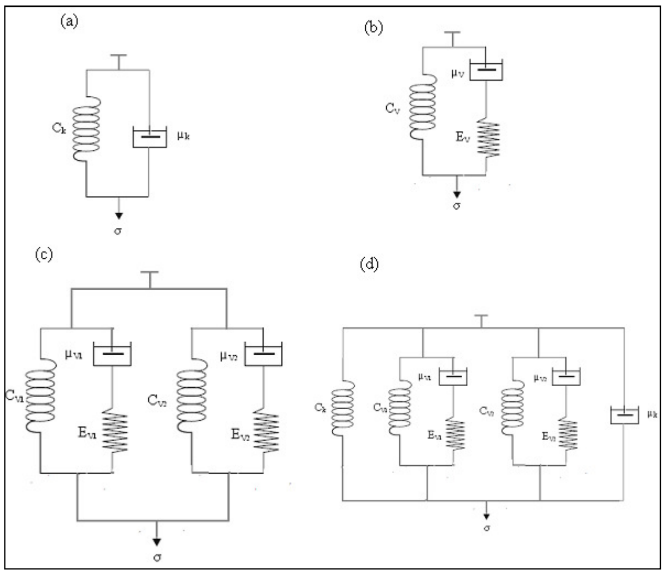

Fig. 5. Experimental and theoretical curves of the tensile test for hydroentangled nonwoven HN1: (a) Kelvin model with nonlinear spring fitting, (b) one-term generalized Vangheluwe model fitting, (c) two-term generalized Vangheluwe model fitting, and (d) combination of Kelvin and Vangheluwe model fitting.

IV. MODEL FITTING

Rheological modeling, based on several mechanistic models for fitting the experimental data of the tensile tests, was investigated to confirm the nonlinear viscoelastic properties of hydroentanglement nonwoven fabrics. The fitting accuracy can be assessed by comparing the coefficient estimation R^2. The closer this coefficient is to 1, the better the fit is. Figure 6 shows an example of results obtained for hydroentangled nonwoven HN1. Table II details the rheological parameter values and the determination coefficient for different models tested with the hydroentangled nonwoven fabric. The R^2 value of 0.999 shows that the combination of Kelvin and Vanghelwue elements presents an excellent fit for hydroentanglement nonwoven behavior. Figure 6 shows the simulation results of the tensile test. It can be concluded that the Vangheluwe model with seven elements fits reasonably well with the experimental results. After calculating the different coefficients of the different rheological models studied (Table II), it can be observed that the combination of Kelvin and Vangheluwe elements simulates the tensile behavior of hydroentangled nonwoven fabrics well and is better than the other models, with an R^2 value of nearly 1.

TABLE II. DETERMINATION OF THE COEFFICIENT PARAMETERS OF THE RHEOLOGICAL MODELS FOR HN1.

Rheological parameters	C_k	μ_k	C_v	E_v	μ_v	R^2
Kelvin model with nonlinear spring	0.0048	0.00611	-	-	-	0.91
One-term generalized Vangheluwe model			0.00066	0.12513	0.65879	0.87
Two-term generalized Vangheluwe model			0.00049	0.05781	0.0409	0.00049
Combination of Kelvin and Vangheluwe model fitting	0.00184	0.00066	0.00184	0.47997	0.1421	0.01184

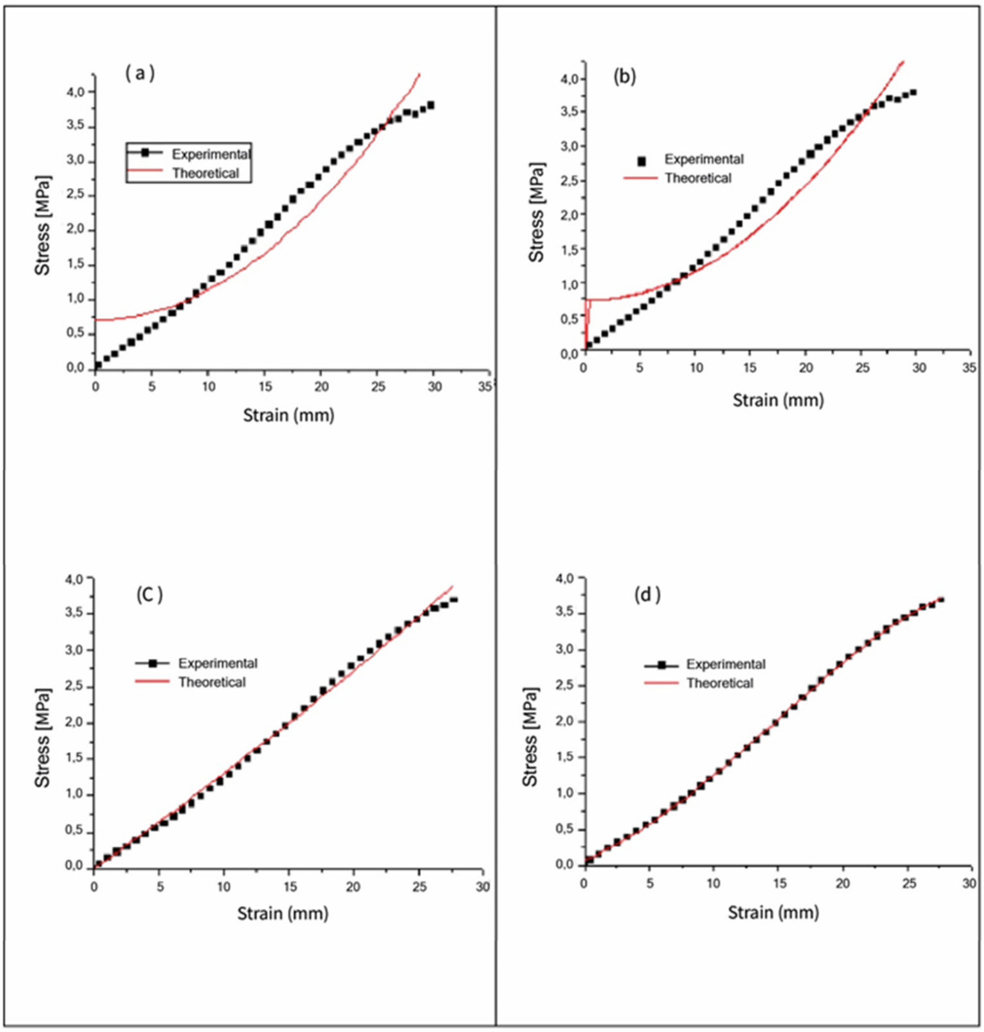

Fig. 6. Experimental and theoretical curves of the tensile test for hydroentanglement nonwoven fabrics.

The experimental values of the tensile curves were simulated to validate the proposed model, describing the tensile behavior of the different hydroentanglement nonwoven fabrics with varied parameters. Figure 6 presents the simulation results. As can be observed, the proposed model goes hand in hand with the experimental data of the tensile tests of hydroentanglement nonwoven fabrics for different compositions and square weights. Therefore, it is confirmed that the model can describe the viscoelastic behavior of hydroentangled nonwoven. Table III indicates the model parameters obtained and the determination coefficient R^2 of different hydroentangled nonwoven fabrics. Figure 6 and Table III show that the experimental curves of the tensile test overlapped with the theoretical curves. The determination coefficient R^2 values are equal to 0.999 for most fabrics. The combination of Kelvin and Vangheluwe elements adjusts well to the experimental tensile data for the hydroentangled nonwoven fabrics. Consequently, the model can be exploited to describe the nonlinear viscoelastic behavior of hydroentangled nonwoven fabrics.

TABLE III. DETERMINATION COEFFICIENT FOR THE TENSILE TEST OF DIFFERENT HYDROENTANGLED NONWOVEN FABRICS.

	Rheological parameters								
Nonwoven composition	C_k	μ_k	C_{v1}	E_{v1}	μ_{v1}	C_{v2}	E_{v2}	μ_{v2}	R^2
HN1	0.00184	0.00066	0.00184	0.47997	0.1421	0.01184	0.55731	0.6455	0.999
HN2	1.00091	0.00007	1.5054	0.08372	9.6131	0.5018	0.0995	8.787	0.999
HN3	0.7975	0.00924	0.05189	0.33208	1.34332	0.11763	1.125	0.00025	0.999
HN4	1.0734	0.0004	1.127	1.4145	1.0983	0.073	1.373	0.986	0.999
HN5	0.4948	0.0001	1.484	0.4239	0.10627	1.0003	0.358	0.1663	0.999
HN6	0.0642	0.0005	0.0899	0.1207	0.04253	0.02998	0.1167	7.3494	0.999
HN7	1.00012	0.00132	1.5007	0.5278	2.6102	0.50025	0.6521	7.09946	0.999
HN8	0.358	0.0006	0.5023	1.4706	0.8534	0.16744	1.4494	0.9996	0.999
HN9	0.0014	0.001	0.0014	0.07538	1.0455	0.0014	0.07952	0.02351	0.999
HN10	0.72766	0.0012	0.9155	0.67285	4.033	0.1948	0.6779	0.5574	0.998
HN11	1.0457	0.0005	1.0445	0.1153	0.4684	0.0012	0.17344	0.1.27814	0.999

V. CONCLUSIONS

There is a lack of accurate rheological models to describe the complex mechanical behavior of hydroentangled nonwoven fabrics under uniaxial loading. To address this knowledge gap, this study investigated four different rheological models, including a novel configuration consisting of a nonlinear spring parallel to a Maxwell element. This study involved deriving mathematical expressions for the proposed model, obtaining the rheological parameters of the nonwoven structure, and calculating the rheological coefficients of the individual structural elements. These values were used to predict the mechanical performance of other nonwoven structures. The results showed that the proposed model accurately predicted the nonlinear viscoelastic behavior of hydroentangled nonwoven fabrics, outperforming existing models. The fitting results of the experimental data with the theoretical equations demonstrated high accuracy in estimating the mechanical trend of the hydroentangled nonwoven structures under uniaxial loading. The significance of this work lies in the development of a more precise rheological model for hydroentangled nonwoven fabrics. This novel approach provides a better understanding of the complex mechanical properties of these materials, which is crucial for their design and application in various industries. This study contributes to current knowledge by offering a generalized model that can be applied to other hydroentangled nonwoven fabrics with specific materials, potentially advancing the field of nonwoven fabric engineering and expanding possibilities for their use in diverse applications.

NOTATIONS

ε: Deformation.

$\acute{\varepsilon}$: Extension rate.

σ: Constraint.

E_v, E_{v1}, E_{v2}: Elasticity modulus of Vangheluwe elements.

μ_v, μ_{v1}, μ_{v2}: Viscosity modulus of Vangheluwe elements.

μ_k: Viscosity modulus of Kelvin elements.

C_v, C_{v1}, C_{v2}: Coefficient of nonlinear spring of Vangheluwe elements.

C_k: Coefficient of nonlinear spring of Kelvin elements.

REFERENCES

[1] F. G. K. Abdulla and R. Abdulla, "A Comparative Application for Evaluating Composite Fabrics Used in Electromagnetic Shielding," *Engineering, Technology & Applied Science Research*, vol. 7, no. 6, pp. 2156–2159, Dec. 2017, https://doi.org/10.48084/etasr.1480.

[2] M. Kanan, B. Wannassi, B. Azouz, M. Ben Hassen, R. Assaf, and A. S. Barham, "Cotton recycling: An experimental study of the mechanical preparation process," *Case Studies in Chemical and Environmental Engineering*, vol. 10, Dec. 2024, Art. no. 100849, https://doi.org/10.1016/j.cscee.2024.100849.

[3] A. Wilsoii, "Development of the nonwovens industry," in *Handbook of Nonwovens*, S. J. Russell, Ed. Cambridge, UK: Woodhead Publishing, 2006.

[4] "Sustainability Report," EDANA, Brussels, Belgium, 2016. [Online]. Available: https://www.edana.org/docs/default-source/sustainability/sustainability-report.pdf?sfvrsn=4a926b0_18.

[5] H. Gaminian, B. Ahvazi, J. J. Vidmar, U. Ekuere, and S. Regan, "Revolutionizing Sustainable Nonwoven Fabrics: The Potential Use of Agricultural Waste and Natural Fibres for Nonwoven Fabric," *Biomass*, vol. 4, no. 2, pp. 363–401, Jun. 2024, https://doi.org/10.3390/biomass4020018.

[6] H. Abidi *et al.*, "Accelerated weathering of textile waste nonwovens used as sustainable agricultural mulching," *Journal of Industrial Textiles*, vol. 50, no. 7, pp. 1079–1110, Feb. 2021, https://doi.org/10.1177/1528083719855326.

[7] M. Halimi, M. Hassen, and B. Wanassi, "Optimization and valorization of recycled fiber in non-woven fabric," *Industria Textila*, vol. 69, pp. 440–445, Jan. 2019, https://doi.org/10.35530/IT.069.06.1534.

[8] O. Gutierrez-Moscardo, M. Canet, J. Gomez-Caturla, D. Lascano, E. Fages, and L. Sanchez-Nacher, "Sustainable materials with high insulation capacity obtained from wastes from hemp industry processed by wet-laid," *Textile Research Journal*, vol. 92, no. 7–8, pp. 1098–1112, Apr. 2022, https://doi.org/10.1177/00405175211046058.

[9] A. Wilson, "The formation of dry, wet, spunlaid and other types of nonwovens," in *Applications of Nonwovens in Technical Textiles*, R. A. Chapman, Ed. Woodhead Publishing, 2010, pp. 3–17.

[10] S. Zannen, M. T. Halimi, M. B. Hassen, E. H. Abualsauod, and A. M. Othman, "Development of a Multifunctional Wet Laid Nonwoven from Marine Waste Posidonia oceanica Technical Fiber and CMC Binder,"

Polymers, vol. 14, no. 5, Feb. 2022, Art. no. 865, https://doi.org/10.3390/polym14050865.

[11] "Nonwoven Fabrics - Chemical Economics Handbook," S&P Global, 2020.

[12] S. Debnath, "13 - Sustainable production and application of natural fibre-based nonwoven," in *Sustainable Fibres and Textiles*, S. S. Muthu, Ed. Woodhead Publishing, 2017, pp. 367–391.

[13] O. B. Berkalp, B. Pourdeyhimi, and A. Seyam, "Texture Evolution in Hydroentangled Nonwovens," *International Nonwovens Journal*, vol. os-12, no. 1, Mar. 2003, https://doi.org/10.1177/1558925003os-1200110.

[14] S. J. Russell, *Handbook of Nonwovens*. Woodhead Publishing, 2022.

[15] A. Watzl and A. Desch, "Spunlace technology for woven fabrics," *International Textile Bulletin-English Edition*, vol. 47, no. 1, pp. 68–70, 2001.

[16] N. Mao and S. J. Russell, "A framework for determining the bonding intensity in hydroentangled nonwoven fabrics," *Composites Science and Technology*, vol. 66, no. 1, pp. 80–91, Jan. 2006, https://doi.org/10.1016/j.compscitech.2005.05.030.

[17] B. Pourdeyhimi, A. Minton, M. Putnam, and H. S. Kim, "Structure-Process-Property Relationships in Hydroentangled Nonwovens -Part 1: Preliminary Experimental Observations," *International Nonwovens Journal*, Dec. 2004, https://doi.org/10.1177/1558925004os-1300403.

[18] E. Ghassemieh, M. Acar, and H. K. Versteeg, "Microstructural analysis of non-woven fabrics using scanning electron microscopy and image processing. Part 2: Application to hydroentangled fabrics," *Proceedings of the Institution of Mechanical Engineers, Part L: Journal of Materials: Design and Applications*, vol. 216, no. 4, pp. 211–218, Oct. 2002, https://doi.org/10.1177/146442070221600401.

[19] P. Xiang, A. V. Kuznetsov, and A. M. Seyam, "Modeling of the Hydroentanglement Process," *Journal of Engineered Fibers and Fabrics*, vol. 1, no. 2, Jun. 2006, https://doi.org/10.1177/155892500600100201.

[20] H. Wang, J. Zhu, X. Jin, and H. Wu, "A Study on the Entanglement and High-Strength Mechanism of Spunlaced Nonwoven Fabric of Hydrophilic PET Fibers," *Journal of Engineered Fibers and Fabrics*, vol. 8, no. 4, Dec. 2013, https://doi.org/10.1177/155892501300800415.

[21] D. Moyo, R. D. Anandjiwala, and A. Patnaik, "Micromechanics of hydroentangled nonwoven fabrics," *Textile Research Journal*, vol. 87, no. 2, pp. 135–146, Jan. 2017, https://doi.org/10.1177/0040517515624877.

[22] A. M. Manich, M. H. Ussman, and A. Barella, "Viscoelastic Behavior of Polypropylene Fibers," *Textile Research Journal*, vol. 69, no. 5, pp. 325–330, May 1999, https://doi.org/10.1177/004051759906900503.

[23] L. Vangheluwe and P. Kiekens, "Modelling Relaxation Behaviour of Yarns Part I: Extended, Nonlinear Maxwell Model," *The Journal of The Textile Institute*, vol. 87, no. 2, pp. 296–304, Jan. 1996, https://doi.org/10.1080/00405009608659082.

[24] H. Helali, B. A. Dhouib, S. Msahli, and M. Cheikhrouhou, "Rheological Modeling of the Dorlastan Core Spun Yarns for Various Dorlastan Drafts and Yarn Counts," *Journal of Textile Science & Engineering*, vol. 3, no. 1, 2013, https://doi.org/10.4172/2165-8064.1000127.

[25] S. Maatoug, N. Ladhari, and F. Sakli, "Viscoelastic Behavior of Starch Sized Warps," *Journal of Applied Sciences*, vol. 7, no. 16, pp. 2376–2379, 2007.

[26] A. M. Manich, P. N. Marino, M. D. de Castellar, M. Saldivia, and R. M. Saurí, "Viscoelastic modeling of natural and synthetic textile yarns," *Journal of Applied Polymer Science*, vol. 76, no. 14, pp. 2062–2067, 2000, https://doi.org/10.1002/(SICI)1097-4628(20000628)76:14<2062::AID-APP9>3.0.CO;2-T.

[27] W. Żurek, M. Chrzanowski, W. Sybilska, and I. Jałmużna, "The application of Zurek's rheological model for description of mechanical behaviour of textiles subjected to different state of loads," *Journal of Achievements in Materials and Manufacturing Engineering*, vol. 43, no. 2, 2010.

[28] N. Halleb and S. B. Amar, "Model modification and prediction of mechanical behaviour of fabrics in uniaxial tension," *The Journal of The Textile Institute*, vol. 101, no. 8, pp. 707–715, Aug. 2010, https://doi.org/10.1080/00405000902812875.

[29] X. Gao, H. Chen, and S. Sun, "Analysis of the Creep Properties of Nonwoven Fabric with Mechanical Models," *Fibres & Textiles in Eastern Europe*, no. Vol. 23, 1 (109), pp. 72–76, 2015.

[30] W. Wiezlak and K. Gniotek, "Indices characterising rheological properties of geo-nowovens during compression," *Fibres & Textiles in Eastern Europe*, vol. 7, no. 3, pp. 40–44, 1999.

[31] I. Krucinska, I. Jalmuzna, and W. Zurek, "Modified Rheological Model for Analysis of Compression of Nonwoven Fabrics," *Textile Research Journal*, vol. 74, no. 2, pp. 127–133, Feb. 2004, https://doi.org/10.1177/004051750407400208.